Published in final edited form as:
J Phys Chem Lett. 2013 May 2; 4(9): 1404–1409. doi:10.1021/jz400438m.

Timescales of Coherent Dynamics in the Light Harvesting Complex 2 (LH2) of *Rhodobacter sphaeroides*

Andrew F. Fidler[1], **Ved P. Singh**[1], **Phillip D. Long**[2], **Peter D. Dahlberg**[2], and **Gregory S. Engel**[1,*]

[1]Department of Chemistry, The James Franck Institute and The Institute for Biophysical Dynamics, The University of Chicago, Chicago, Illinois 60637, USA

[2]Program in the Biophysical Sciences, The University of Chicago, Chicago, IL 60637

Abstract

The initial dynamics of energy transfer in the light harvesting complex 2 from *Rhodobacter sphaeroides* were investigated with polarization controlled two-dimensional spectroscopy. This method allows only the coherent electronic motions to be observed revealing the timescale of dephasing among the excited states. We observe persistent coherence among all states and assign ensemble dephasing rates for the various coherences. A simple model is utilized to connect the spectroscopic transitions to the molecular structure, allowing us to distinguish coherences between the two rings of chromophores and coherences within the rings. We also compare dephasing rates between excited states to dephasing rates between the ground and excited states, revealing that the coherences between excited states dephase on a slower timescale than coherences between the ground and excited states.

Keywords

Spectroscopy; Excited States; Biophysics; Dynamics

Understanding the molecular mechanisms underpinning energy transfer events in photosynthetic complexes has been of long standing interest, for both technological and pedagogical purposes.[1–3] The light harvesting complex 2 (LH2), a peripheral antenna complex from purple bacteria, has been heavily studied by a wide variety of experimental and theoretical techniques.[4–6] The LH2 complex is composed of 27 bacteriochlorophyll a chromophores arranged circularly in two concentric rings, shown in Figure 1.[7] The inner ring contains eighteen strongly interacting chromophores known as the B850 chromophores due to their prominent absorption at 850 nm. The outer ring of nine more weakly interacting chromophores comprises the B800 ring, which contribute to the absorption at 800 nm. A large variety of spectroscopic methods have successfully mapped out the energy landscape[8, 9], the timescales of the relaxation dynamics following photoexcitation,[10, 11] as well as characterizations of the electronic environment of the surrounding protein.[12, 13] Detailed modeling of these various experiments has allowed for a detailed understanding of the dynamics, however the experimental energy transfer timescales can be reproduced by both modified Redfield theories as well as multichromophoric Förster resonance energy

*To whom correspondence should be addressed. gsengel@uchicago.edu.

Supporting Information Available: Complete details of the model and parameters used to simulate the linear absorbance spectrum are provided. This material is available free of charge via the Internet at http://pubs.acs.org.

transfer (FRET).[14–16] These two models provide strikingly different pictures of the underlying dynamics.

More recently the question of the presence of coherent electronic motion in this system has started to be addressed, which may help distinguish the more correct relaxation mechanism. A model that is consistent with a wide variety of spectroscopic observables revealed that the fast decay in pump probe anisotropy experiments conducted on the 800 nm region of the spectrum could be attributed to excitonic dephasing, as opposed to relaxation dynamics as previously assigned.[14] This result indicates that energy transfer between the relatively weakly interacting chromophores in the B800 ring may not be adequately described by a FRET like mechanism as had been formerly thought. Two-dimensional electronic spectroscopy (2DES) experiments have observed coherent oscillations between regions of the two broad absorption bands, revealing a rich interplay between the dephasing dynamics and coherent electronic motion.[17] The persistence of coherent electronic motion has now been observed in a wide variety of photosynthetic complexes,[18–21] suggesting that it may be a common feature present in these systems.

In this letter, we extend the previous results through a coherence specific variant of two-dimensional spectroscopy. By controlling the polarization of the incident laser pulses, we selectively detect signals which evolve as a coherence (superposition) between two states with differing dipole moment directions.[22–24] This particular method is well suited to studying coherent evolution which is difficult to distinguish with other methodologies such as pump-probe spectroscopy. Two color photon echo techniques[19, 25] as well as pump-probe anisotropy methods[14, 26] and two-dimensional experiments[18] are also strong probes of coherent dynamics. The coherence-specific polarization scheme has been implemented previously to study the molecular structure of a small dipeptide in solution[22] as well as coherent dynamics in the LHCII complex of photosystems II[24] and the reaction center of purple bacteria.[27] The coherence specific polarization sequence is given by $\pi/4$, $-\pi/4$, $\pi/2$, and 0 radians for pulses one, two, three, and the local oscillator, respectively.[22] Coherences involving states with parallel or anti-parallel transition dipoles cannot be observed with this methodology. Coherent vibrational motion could also contribute to this signal, provided that the transition dipole direction is dependent on nuclear coordinates. Such non-Condon effects have been observed in photosynthetic antenna complexes containing phycocyanobilin pigments, where high frequency out-of-plane vibrational modes were measured in transient absorption anisotropy experiments.[28]

To acquire the coherence-specific data, we utilize a single-shot variant of 2DES called GRadient Assisted Photon Echo (GRAPE) spectroscopy.[29, 30] In this experiment, we create a temporal gradient between the first two pulses across a homogeneous sample. An imaging spectrometer captures and resolves the temporal gradient thereby acquiring an entire two-dimensional map in parallel. GRAPE reduces the need for long term phase stability and power stability by reducing the acquisition time by two orders of magnitude. The inclusion of three half-wave plates in the paths of beams 1–3 allows complete control of the polarization pulse sequence. We generate broadband optical pulses by focusing the output of a regenerative amplifier into Argon at ~1.3 atm generating spectrally broadened pulses centered at 800 nm with ~ 100 nm of bandwidth. This spectrally broadened pulse was compressed with an SLM based pulse shaper (Biophotonics Solutions) to 15 fs (FWHM). The waiting time was sampled from −100 to 500 fs in 10 fs steps. The sample was isolated and prepared as previously described.[31] The peak absorbance at 850 nm was ~0.2 OD in a 200 μm length cell. All experiments were conducted at room temperature. Due to uncertainties in the relative phases of our excitation pulses, we report only the absolute value of our signal. The GRAPE spectrometer acquires only the rephasing portion of the third order optical response.

The coherence-specific 2D spectra are shown in Figure 2. At early waiting times, the presence of signal simply reveals the presence of a superposition state. The identity of the coherence can be determined by examining the location of the signal in the 2D map, and the dephasing of that particular coherence is resolved by examining the signal with increasing waiting time. Two diagonal features are resolved, corresponding to the two bands centered at 850 nm and 800 nm in the linear absorption spectrum. The spectra show intense features on the diagonal even though theory predicts the rephasing portion of the coherence signal to be located off the diagonal. We attribute this shift to dispersive contributions to the signal, which broaden the peaks in the absolute value of the signal. Cross-peaks between the two main features are also clearly resolved. As the waiting time is increased, the system relaxes due to interactions between the chromophores and the surrounding protein matrix, spurring dephasing. The signal rapidly decays with increasing waiting time, most predominantly in the lower energy band and cross peaks between the two bands. Unlike the conventional all parallel polarization scheme, contributions from populations are highly suppressed in the coherence-specific scheme allowing us to directly Fourier transform the full complex data. In this fashion, we can distinguish positive from negative frequencies. Traces of the Fourier transforms of the cross peak between the features at 800 nm and 834 nm reveal frequencies centered at the difference between the axes and rotating in opposite directions. This effect is not predicted by the theory of a purely vibrational coherence, leading us to conclude that the coherence is of an electronic origin.[32, 33] The magnitudes of the traces are roughly equal and are consistent with theoretical predictions. Integration over the λ_τ and λ_t domains reveals the average timescales of dephasing present in the system.[24] The total signal undergoes a fast initial decay followed by a slower decay, with the signal nearly vanishing by 500 fs. The signal is well modeled by the sum of a Gaussian, exponential, and constant offset. The parameters of the fit are listed in table 1.

We have utilized a Frenkel-excitonic framework to model the absorption spectrum of the complex and to connect the spectroscopic signatures to the molecular structure. Material parameters for the site energies, couplings, and spectral densities were taken from previous studies of the complex.[12, 13, 15, 34] Complete details of the model are provided in the supplemental information section. Our model provides a reasonable fit to both the absorption spectrum of the native complex as well as a modified complex which lacks the B800 chromophores. We then classify states based on their probability amplitude and group states into three categories. The first two categories are states that are > 90% localized on either the B850 or B800 chromophores, and the third category is comprised of states that are delocalized across both rings. Calculations of the absorption spectrum of these states then reveals that the B850 pigments largely absorb at 850 nm along with a lower wavelength tail that extends past the 800 nm feature. The 800 nm region of the spectrum is predominantly comprised of excitations that are localized on the B800 pigments or mixed states involving both rings of chromophores, in agreement with previous studies.[14]

Two-dimensional slices through different values of λ_τ are shown in Figure 3. We see that coherent oscillations occur throughout the entire spectral region and closely follow the energy difference between the axes. A slice through λ_τ = 774 nm reveals that coherence is maintained between the highest energy region of the 800 nm band and the 850 nm band. This coherence can be definitively assigned to coherence between lower and higher lying electronic excitations on the inner B850 ring. Lower frequencies within the 850 nm region are also observed, revealing that coherence within the B850 chromophores is maintained at short times. Because the contribution to the absorbance at 800 nm from the B850 chromophores is minor, we preliminarily attribute this feature to the B800 chromophores. This assignment is strengthened by the significantly smaller intensity of the signal in the lower wavelength region which we can unambiguously attribute to the B850 ring. Our data reveals that the coherent signal is more intense within the individual absorption bands, but a

weaker signal is still present connecting the two bands. The timescales that we extract are in reasonable agreement with previous studies conducted at 77 K. For the 800 nm region, the 177 fs decay that we observe at room temperature is faster than the 300 – 500 fs timescale extracted from anisotropy experiments which were conducted at 77 K.[14] Similarly, the initial decay of anisotropy within the 850 nm region at 77 K was found to be significantly faster with a timescale of roughly 60 fs compared with our Gaussian decay time of 15 fs from our experiment. The increased temperature, yielding amplified thermal motion, most likely explains the increased dephasing rates.

A complete simulation of the dephasing dynamics would require consideration of the full nonlinear response, which is non-trivial. Instead, we present a minimal theoretical framework to provide a qualitative understanding of the measured dynamics. Within the secular approximation, which decouples populations and coherences, we can approximate the evolution of the coherence between excited states *i* and *j* with the following equation:[35–37]

$$\rho_{ji}(t) \propto \langle \exp\left[-i\omega_{ji}t - g_{jj}(t) - g_{ii}(t) + 2Re\left(g_{ij}(t)\right) - (k_j + k_i)t\right]\rangle. \quad (1)$$

Here ω_{ij} is the difference in energy between the states *i* and *j* divided by the reduced Planck's constant, $g_{jj}(t)$ is the lineshape function which describes the dephasing induced by interactions with the bath for state *j*, $g_{ij}(t)$ is the lineshape function which describes the extent to which the fluctuations induced by the bath between the states *i* and *j* are correlated, and k_i is the rate of population loss of the state *i*. The angular brackets indicate an average over disorder in the system, reflecting the ensemble nature of the measurement. The dynamics of this coherence between excited states differs from the observed dynamics of the coherence between the ground state and excited state *j*, which can be approximated by:[35–37]

$$\rho_{jg} \propto \langle \exp\left[-i\omega_{jg} - g_{jj}(t) - k_j t\right]\rangle. \quad (2)$$

Here, ω_{jg} is the transition energy between the ground state and the j_{th} excited state. Comparing these two equations reveals that the interactions governing the dephasing of coherences between excited states and coherence between the ground and excited states are largely shared, differing only to the extent that fluctuations (either static disorder or dynamic disorder) are correlated. Correlated fluctuations can arise from excitonic mixing between states as well as from correlated environmental motions.[19] Due to the strong interactions between chromophores in the LH2 complex, the dominant contribution to the correlated fluctuations most likely arises from simply excitonic mixing. The electronic states involving the B850 chromophores are highly delocalized across ~4–5 chromophores at room temperature.[4] Recent calculations utilizing the hierarchical equations of motion found the presence of coherent electronic motion within the B850 chromophores persisting on a 150 fs timescale at room temperature for a single realization of the Hamiltonian (i.e. neglecting disorder in the system).[38] This result suggests that the strong coupling which yields delocalized excitations is the physical mechanism that yields persistent coherent motion on the excited state and confirms that coherence persists longer in a single system when compared to ensemble measurements. Similarly, the 77 K pump-probe anisotropy measurements could also be reproduced without assuming correlated spectral motion.[14] We can experimentally measure the dephasing of the ground and excited state coherences through separately acquired all parallel polarization 2DES. Traces through coherence time τ at different emission wavelengths λ_t then reveal the dephasing dynamics of the ground excited state coherences. This signal is equivalent to a wavelength resolved three pulse photon echo peak shift experiment.[39] We compare the dephasing dynamics between these two classes of coherences in figure 4.

The all parallel 2DES signal oscillates at an optical frequency and fully decays by 150 fs. This dephasing time is rather long when compared to most small molecules in solution at room temperature, which typically dephase by 50 fs. A defining characteristic of protein environments seems to be reduced coupling to the environment.[40] The maximum of the signal is shifted from a coherence time of zero due to inhomogeneity present and the rephasing process of a photon echo. The recovered shift of 31 fs is in good agreement with previous measurements.[39] The coherence-specific signal shows a similar short 31 fs timescale, as well as a longer lived 177 fs exponential decay, shown by both the integrated intensity and individual traces. The short timescale is associated with coherence between the states at 800 and 850 nm as well as states within the 850 nm band. The longer lived coherence is primarily located within the 800 nm feature, though weaker long-lived features are also present within the 850 nm feature. The lifetime extracted in the coherence-specific experiment is shorter than the previously reported timescale extracted from an all parallel polarization 2DES experiment due to our increased temporal resolution.[17]

It is somewhat counter intuitive that coherence persists longer among the more weakly bound chromophores rather than the more strongly interacting chromophores. We interpret this paradox as arising from the ensemble nature of our experiment, meaning the ensemble measurement likely differs from measurements of individual members of the ensemble. Previous photon echo peak shift measurements of the 800 nm and 850 nm spectral regions have revealed that the protein environments are distinct between the two absorption bands.[12, 13] The 800 nm spectral region has a reduced overall coupling strength to the bath, on both ultrafast timescales and slower timescales. The slower timescales, present in most proteins, lead to strong wavelength dependence of the beating observed in Figure 3. This ensemble inhomogeneity leads to an artificial dephasing in our measurement that would not be present if decoherence in a single protein complex was measured.[41–43] Because the 850 nm spectral region is more inhomogeneous, these slower timescales will most likely lead to an increased dephasing rate. Thus coherence persists longer than the timescale measured in this experiment, and furthermore, the dephasing rate in the 850 nm region is artificially shortened to a greater degree. Although we cannot recover the true decoherence timescale with the current technique without making assumptions to the magnitude of shared fluctuations in equation (1), we do know that our measurement represents a lower bound for the coherence lifetime. We can then compare this lifetime to the coherence lifetime between ground and excited states. We measure the coherence lifetime between ground and excited states using the rephasing process of photon echo signals, which represents an accurate measure of the decoherence time because the echo signal and is largely free from inhomogeneous artifacts. We conclude that coherence among excited states persists on a longer timescale than coherence between the ground and excited states, indicating a strong correlation between the electronic states.

Utilizing the coherence-specific polarization sequence, we directly observe coherences among all excited states. The persistence of coherence between all states indicates that a purely FRET based model is not consistent with describing the energy transfer dynamics in this system. Due to the inhomogeneous nature of the protein and the rephasing capability of the photon echo signals, we conclude that excited state coherences persist longer than coherences between the ground and excited states. The background-free detection of excited state coherence clarifies the observation of lower frequency oscillations as well as the distinction between positive and negative frequencies, revealing results consistent with excitonic theory.

Supplementary Material

Refer to Web version on PubMed Central for supplementary material.

Acknowledgments

The authors thank NSF MRSEC (DMR 08-02054), AFOSR (FA9550-09-1-0117), and the DARPA QuBE program (N66001-10-1-4060) for partially supporting this work. A.F.F. and P.D.L. thank the DOE SCGF program for funding. P.D.D. was supported by the Graduate Program in Biophysical Sciences at the University of Chicago (National Institutes of Health grant T32 EB009412).

References

1. van Amerongen, H.; Valkunas, L.; van Grondelle, R. Photosynthetic Excitons. Singapore: World Scientific; 2000.
2. Blankenship, R. Molecular Mechanisms of Photosynthesis. Oxford: Blackwell Science; 2002.
3. Scholes GD, Fleming GR, Olaya-Castro A, van Grondelle R. Lessons from nature about solar light harvesting. Nat. Chem. 2011; 3:763–774. [PubMed: 21941248]
4. Sundstrom V, Pullerits T, van Grondelle R. Photosynthetic light-harvesting: Reconciling dynamics and structure of purple bacterial LH2 reveals function of photosynthetic unit. J. Phys. Chem. B. 1999; 103:2327–2346.
5. van Grondelle R, Novoderezhkin VI. Energy transfer in photosynthesis: experimental insights and quantitative models. Phys. Chem. Chem. Phys. 2006; 8:793–807. [PubMed: 16482320]
6. Cogdell RJ, Gall A, Kohler J. The architecture and function of the light-harvesting apparatus of purple bacteria: from single molecules to in vivo membranes. Q. Rev. Biophys. 2006; 39:227–324. [PubMed: 17038210]
7. McDermott G, Prince SM, Freer AA, Hawthornthwaitelawless AM, Papiz MZ, Cogdell RJ, Isaacs NW. Crystal-Structure of an Integral Membrane Light-Harvesting Complex from Photosynthetic Bacteria. Nature. 1995; 374:517–521.
8. Monshouwer R, Abrahamsson M, vanMourik F, vanGrondelle R. Superradiance and exciton delocalization in bacterial photosynthetic light-harvesting systems. J. Phys. Chem. B. 1997; 101:7241–7248.
9. Chachisvilis M, Kuhn O, Pullerits T, Sundstrom V. Excitons in photosynthetic purple bacteria: Wavelike motion or incoherent hopping? J. Phys. Chem. B. 1997; 101:7275–7283.
10. Shreve AP, Trautman JK, Frank HA, Owens TG, Albrecht AC. Femtosecond Energy-Transfer Prpcesses in the B800–850 Light-Harvesting Complex of Rhodobacter-Sphaeroides-2.4.1. Biochim. Biophys. Acta. 1991; 1058:280–288. [PubMed: 2049375]
11. Hess S, Feldchtein F, Babin A, Nurgaleev I, Pullerits T, Sergeev A, Sundstrom V. Femtosecond Energy-Transfer Within The LH2 Peripheral Antenna of The Photosynthetic Purple Bacteria Rhodobacter-Sphaeroides and Rhodopseudomonas-Palustris LL. Chem. Phys. Lett. 1993; 216:247–257.
12. Jimenez R, vanMourik F, Yu JY, Fleming GR. Three-pulse photon echo measurements on LH1 and LH2 complexes of Rhodobacter sphaeroides: A nonlinear spectroscopic probe of energy transfer. J. Phys. Chem. B. 1997; 101:7350–7359.
13. Joo TH, Jia YW, Yu JY, Jonas DM, Fleming GR. Dynamics in isolated bacterial light harvesting antenna (LH2) of Rhodobacter sphaeroides at room temperature. J. Phys. Chem. 1996; 100:2399–2409.
14. Novoderezhkin V, Wendling M, van Grondelle R. Intra- and interband transfers in the B800–B850 antenna of Rhodospirillum molischianum: Redfield theory modeling of polarized pump-probe kinetics. J. Phys. Chem. B. 2003; 107:11534–11548.
15. Scholes GD, Fleming GR. On the mechanism of light harvesting in photosynthetic purple bacteria: B800 to B850 energy transfer. J. Phys. Chem. B. 2000; 104:1854–1868.
16. Jang S, Newton MD, Silbey RJ. Multichromophoric forster resonance energy transfer from B800 to B850 in the light harvesting complex 2: Evidence for subtle energetic optimization by purple bacteria. J. Phys. Chem. B. 2007; 111:6807–6814. [PubMed: 17439170]
17. Harel E, Engel GS. Quantum coherence spectroscopy reveals complex dynamics in bacterial light-harvesting complex 2 (LH2). Proc. Natl. Acad. Sci. U. S. A. 2012; 109:706–711. [PubMed: 22215585]

18. Engel GS, Calhoun TR, Read EL, Ahn TK, Mancal T, Cheng YC, Blankenship RE, Fleming GR. Evidence For Wavelike Energy Transfer Through Quantum Coherence in Photosynthetic Systems. Nature. 2007; 446:782–786. [PubMed: 17429397]
19. Lee H, Cheng YC, Fleming GR. Coherence dynamics in photosynthesis: Protein protection of excitonic coherence. Science. 2007; 316:1462–1465. [PubMed: 17556580]
20. Calhoun TR, Ginsberg NS, Schlau-Cohen GS, Cheng YC, Ballottari M, Bassi R, Fleming GR. Quantum Coherence Enabled Determination of the Energy Landscape in Light-Harvesting Complex II. J. Phys. Chem. B. 2009; 113:16291–16295. [PubMed: 20014871]
21. Collini E, Wong CY, Wilk KE, Curmi PMG, Brumer P, Scholes GD. Coherently Wired Light-Harvesting in Photosynthetic Marine Algae at Ambient Temperature. Nature. 2010; 463:644–647. [PubMed: 20130647]
22. Zanni MT, Ge NH, Kim YS, Hochstrasser RM. Two-dimensional IR spectroscopy can be designed to eliminate the diagonal peaks and expose only the crosspeaks needed for structure determination. Proc. Natl. Acad. Sci. U. S. A. 2001; 98:11265–11270. [PubMed: 11562493]
23. Abramavicius D, Voronine DV, Mukamel S. Unravelling coherent dynamics and energy dissipation in photosynthetic complexes by 2D spectroscopy. Biophys. J. 2008; 94:3613–3619. [PubMed: 18192357]
24. Schlau-Cohen GS, Ishizaki A, Calhoun TR, Ginsberg NS, Ballottari M, Bassi R, Fleming GR. Elucidation of the timescales and origins of quantum electronic coherence in LHCII. Nat. Chem. 2012; 4:389–395. [PubMed: 22522259]
25. Richards GH, Wilk KE, Curmi PMG, Quiney HM, Davis JA. Coherent Vibronic Coupling in Light-Harvesting Complexes from Photosynthetic Marine Algae. J. Phys. Chem. Lett. 2012; 3:272–277.
26. Savikhin S, Buck DR, Struve WS. Oscillating anisotropies in a bacteriochlorophyll protein: Evidence for quantum beating between exciton levels. Chem. Phys. 1997; 223:303–312.
27. Westenhoff S, Palecek D, Edlund P, Smith P, Zigmantas D. Coherent Picosecond Exciton Dynamics in a Photosynthetic Reaction Center. J. Am. Chem. Soc. 2012; 134:16484–16487. [PubMed: 23009768]
28. Womick JM, West B, Scherer NF, Moran AM. Vibronic effects in the spectroscopy and dynamics of C-phycocyanin. J. Phys. B: At., Mol. Opt. Phys. 2012; 45:12.
29. Harel E, Fidler AF, Engel GS. Real-time mapping of electronic structure with single-shot two-dimensional electronic spectroscopy. Proc. Natl. Acad. Sci. U. S. A. 2010; 107:16444–16447. [PubMed: 20810917]
30. Harel E, Fidler AF, Engel GS. Single-Shot Gradient-Assisted Photon Echo Electronic Spectroscopy. J. Phys. Chem. A. 2011; 115:3787–3796. [PubMed: 21090733]
31. Frank HA, Chadwick BW, Oh JJ, Gust D, Moore TA, Liddell PA, Moore AL, Makings LR, Cogdell RJ. Triplet Triplet Energy-Transfer in B800–850 Light-Harvesting Complexes of Photosynthetic Bacteria and Synthetic Carotenoporphyrin Molecules Investigated by Electron-Spin-Resonance. Biochim. Biophys. Acta. 1987; 892:253–263.
32. Turner DB, Dinshaw R, Lee KK, Belsley MS, Wilk KE, Curmi PMG, Scholes GD. Quantitative investigations of quantum coherence for a light-harvesting protein at conditions simulating photosynthesis. Phys. Chem. Chem. Phys. 2012; 14:4857–4874. [PubMed: 22374579]
33. Butkus V, Zigmantas D, Valkunas L, Abramavicius D. Vibrational vs. electronic coherences in 2D spectrum of molecular systems. Chem. Phys. Lett. 2012; 545:40–43.
34. Krueger BP, Scholes GD, Fleming GR. Calculation of couplings and energy-transfer pathways between the pigments of LH2 by the ab initio transition density cube method. J. Phys. Chem. B. 1998; 102:5378–5386.
35. Adolphs J, Renger T. How proteins trigger excitation energy transfer in the FMO complex of green sulfur bacteria. Biophys. J. 2006; 91:2778–2797. [PubMed: 16861264]
36. Christensson N, Kauffmann HF, Pullerits T, Mancal T. Origin of Long-Lived Coherences in Light-Harvesting Complexes. J. Phys. Chem. B. 2012; 116:7449–7454. [PubMed: 22642682]
37. Fidler AF, Caram JR, Hayes D, Engel GS. Towards a coherent picture of excitonic coherence in the Fenna-Matthews-Olson complex. J. Phys. B: A., Mol. Opt. Phys. 2012; 45:10.

38. Yeh SH, Zhu J, Kais S. Population and coherence dynamics in light harvesting complex II (LH2). J. Chem. Phys. 2012; 137:9.

39. Book LD, Ostafin AE, Ponomarenko N, Norris JR, Scherer NF. Exciton delocalization and initial dephasing dynamics of purple bacterial LH2. J. Phys. Chem. B. 2000; 104:8295–8307.

40. Jordanides XJ, Lang MJ, Song XY, Fleming GR. Solvation dynamics in protein environments studied by photon echo spectroscopy. J. Phys. Chem. B. 1999; 103:7995–8005.

41. Ishizaki A, Fleming GR. On the Interpretation of Quantum Coherent Beats Observed in Two-Dimensional Electronic Spectra of Photosynthetic Light Harvesting Complexes. J. Phys. Chem. B. 2011; 115:6227–6233. [PubMed: 21488648]

42. Fidler AF, Harel E, Long PD, Engel GS. Two-Dimensional Spectroscopy Can Distinguish between Decoherence and Dephasing of Zero-Quantum Coherences. J. Phys. Chem. A. 2012; 116:282–289. [PubMed: 22191993]

43. Pelzer KM, Griffin GB, Gray SK, Engel GS. Inhomogeneous dephasing masks coherence lifetimes in ensemble measurements. J. Chem. Phys. 2012; 136:6.

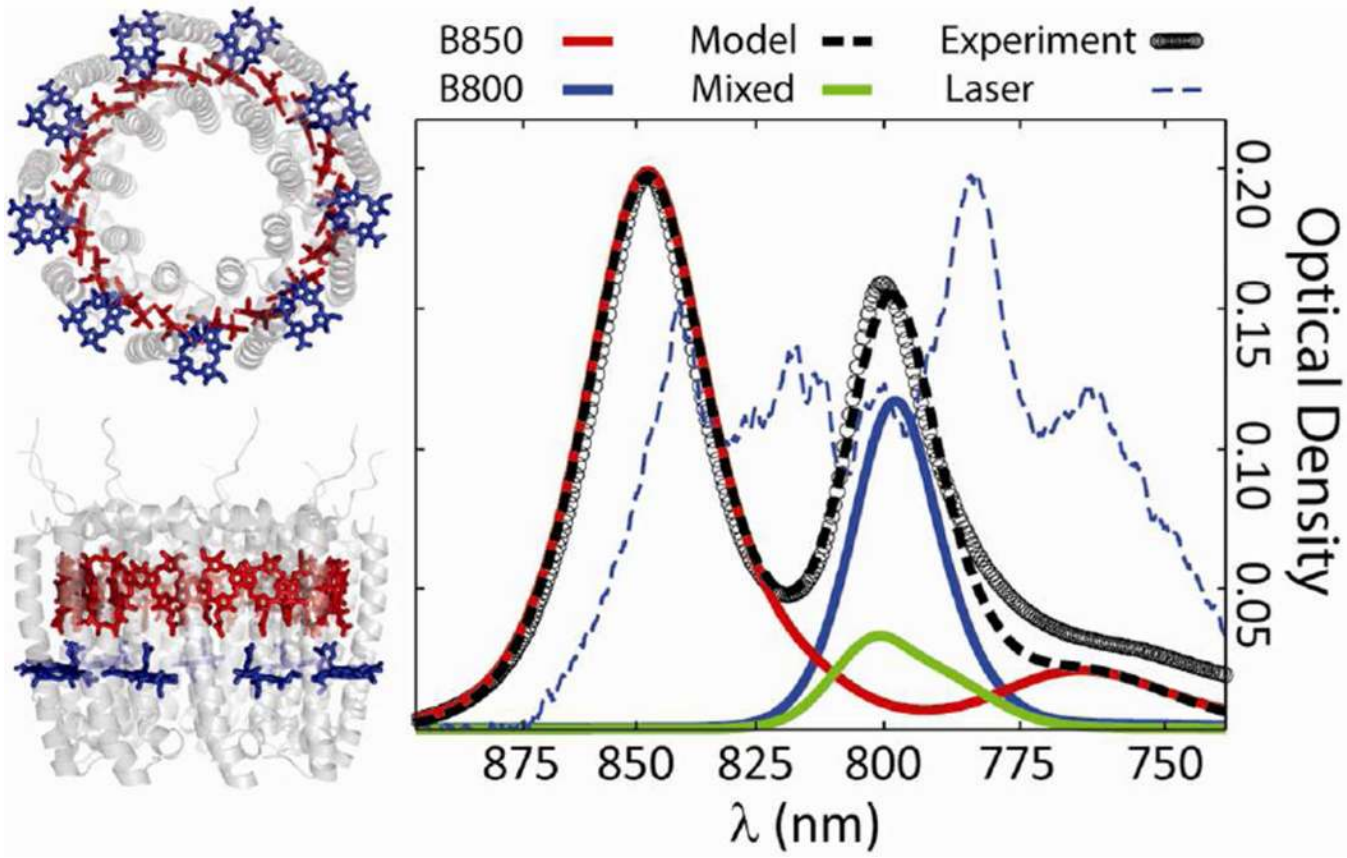

Figure 1.
Crystal structure of the LH2 protein complex (left) with the B850 pigments in red and B800 pigments in blue. Experimental absorption spectrum (black circles) of the LH2 complex and model (black dashed). The theoretical model can be decomposed into contributions from the B850 pigments (red), B800 pigments (blue) and mixed character states (green). The experimental spectrum of the laser pulse is also shown (dashed blue).

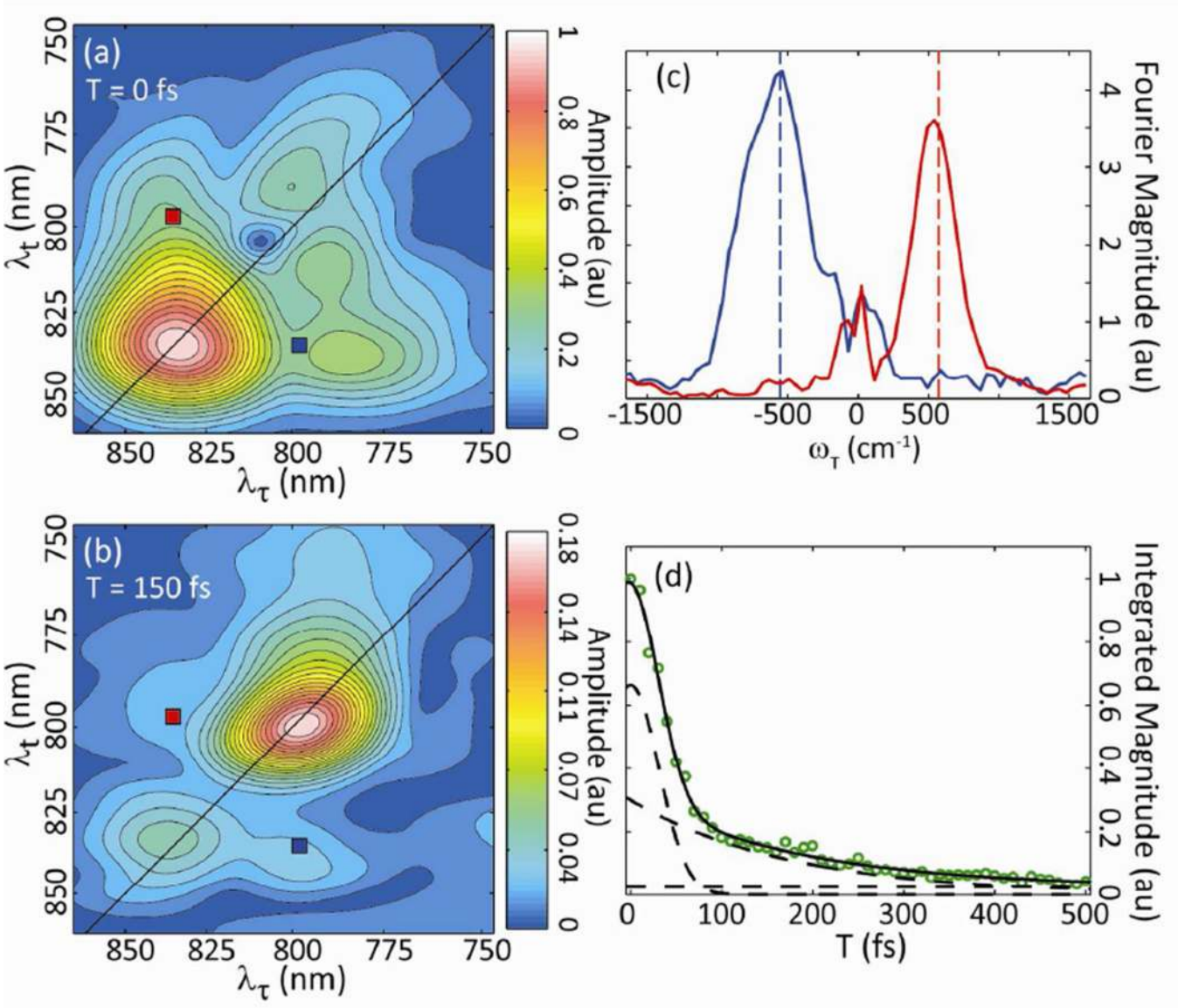

Figure 2.

Absolute value coherence-specific 2D spectra at waiting times of 0 fs (a) and 150 fs (b). A Fourier transform through the cross peaks between 800 nm and 834 nm shows frequencies matching the energy difference between these states. The cross peaks acquire phase in opposite directions (c), consistent with the exciton theory. The total integrated intensity reveals dephasing occurs on two timescales and is well modeled by the sum of a Gaussian and exponential along with a constant offset, whose components are shown in dashed lines (d).

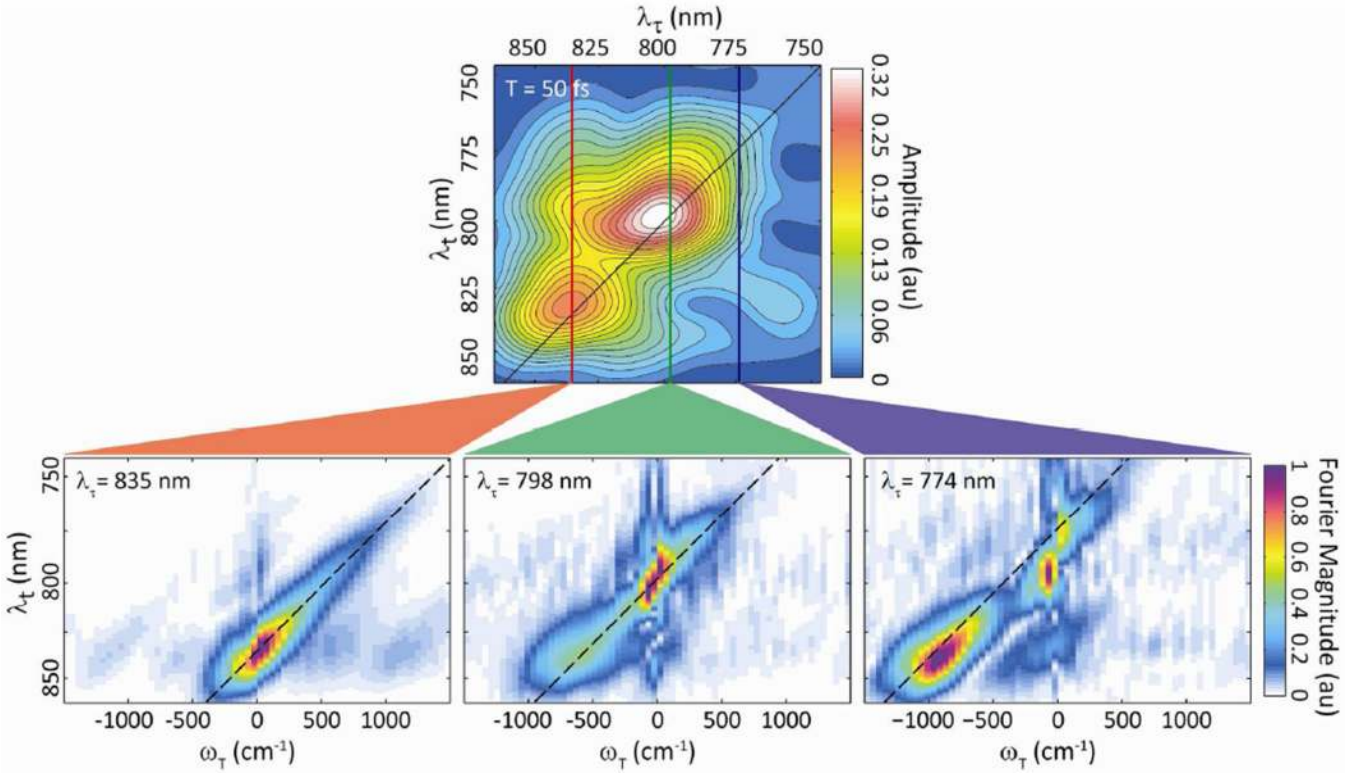

Figure 3.

A coherence-specific spectrum at a waiting time of 50 fs (top). Fourier transforms of slices through the spectrum are taken at λ_τ values of 835 nm, 798 nm, and 774 nm, reveal coherent oscillations throughout the spectrum (bottom). A dashed line is drawn on the line $\omega_T = 2\pi c\left(\frac{1}{\lambda_t} - \frac{1}{\lambda_\tau}\right)$ which closely follows the location of the maximum of the signal.

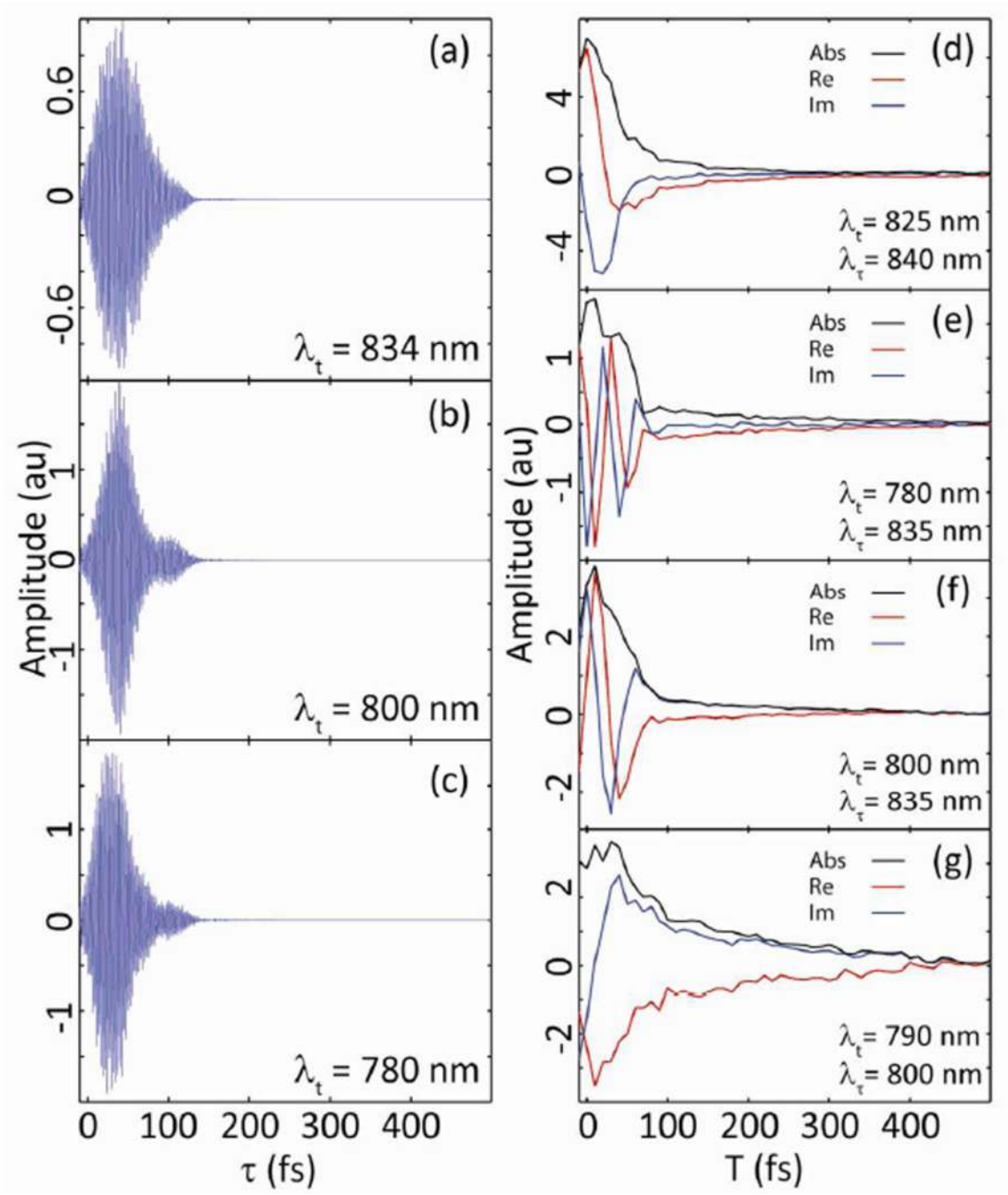

Figure 4.
Comparison of the dephasing of cohereces between the ground and excited state from all parallel poralaizaion 2DES at waiting time of 0 fs (a–c). The real (red), imaganiry (blue), and absolute value (black) of the coherence-specific signal taken at the indicated position (d–g).

Table 1:

List of regression parameters determined to fit the integrated coherence specific intensity.

A_{Gauss}	τ_{Gauss}	A_{exp}	τ_{exp}	C
0.66±0.03	31±1 fs	0.30±0.02	177±32 fs	0.03±0.01